



**Short-chain amino acids functionalized cellulose nanofibers
composite ultrafiltration membrane with enhanced
properties**

Journal:	<i>RSC Advances</i>
Manuscript ID	RA-ART-06-2016-014696.R1
Article Type:	Paper
Date Submitted by the Author:	20-Jul-2016
Complete List of Authors:	<p>Qin, Dujian; Beijing Institute of Technology, Materials science and engineering Zhang, Dalun; Beijing Institute of Technology, School of Materials Sciences & Engineering Shao, Ziqiang; 1. Beijing Institute of Technnology, School of Materials Science and Engineering Beijing Wang, Jianquan; Beijing Institute of Technology, School of Materials Science and Engineering; Tokyo Institute of Technology, Department of Chemistry and Materials Science Mu, Keguang; Beijing Institute of Technology, Department of Materials Science and Engineering liu, yanhua; North Century Cellulose Technology Research & Development. Co. LTD, zhao, libin; Sichuan Nitrocell Co., Ltd</p>
Subject area & keyword:	Films/membranes < Materials

ARTICLE

Cit
e
thi
s:
DO
I:
10.
10
39/
x0
xx
00
00
0x

Short-chain amino acids functionalized cellulose nanofibers composite ultrafiltration membrane with enhanced properties

Dujian Qin,^a Dalun Zhang,^{* a, b} Ziqiang Shao,^{a, b} Jianquan Wang,^{a, b} Keguang Mu^a

Yanhua liu,^c libin Zhao,^d

TEMPO-oxidized cellulose nanofibers (TOCNs) were blended with cellulose acetate (CA) to fabricate high water flux ultrafiltration membrane. In order to further reduce the fouling behavior of membrane, short-chain amino acids were selected as modifiers to graft onto membrane surface. Some properties of modified membranes had been changed such as penetrability, contact angle, zeta potential, anti-fouling and mechanical properties. It was observed that the water flux of TOCNs composite membrane raised from 11.8 l/m²h to 123.4 l/m²h, over 10 times increment compared with unmodified CA membrane. As reinforcing nanofibers, TOCNs also have positive impact for modified membrane on mechanical property. The tensile strength and elongation at break of composite membrane were increased by 23.9% and 40.4%, respectively. After short-chain amino acids modification, little or even no variation had been found in cross-section morphology and pores structure of membrane. The flux recovery ratio (FRR) of lysine modified membrane was increased from 80.0% to 95.9%, while irreversible fouling loss (R_{ir}) decreased from 20% to 4.1%. Grafting lysine onto membrane effectively improved the resistance to protein fouling of membrane, without sacrificing water flux and mechanical properties.

Received 00th January 2012,
Accepted 00th January 2012

DOI: 10.1039/x0xx00000x

www.rsc.org/

1. Introduction

In recent years, the rapid growth of bio-separation has increased the demand for efficient and large-scale purification process of protein.^[1-3] Ultrafiltration membrane technology is an attractive alternative^[4] to conventional energy-intensive separation because of its outstanding high throughput and low process cost. As the petroleum based products, most polymers membranes have to face environmental problems during the production and non-biodegradable problems in the disposal stages of their life cycle. Therefore, using renewable resources to fabricate membranes can create a financial and environmental protection position of competitive benefit. Cellulose acetate (CA), which is renewable, cheap and remarkably biocompatible,^[5] have been used to fabricate ultrafiltration membrane since the 1960s. Subsequently, intensive researches have confirmed the reliability of CA ultrafiltration membrane in micro-solutes purification.^[6] However, CA membranes usually have lower porosity of sub-layer and dense top layer, resulting in low water flux at separation,^[7] and the propensity of proteins to foul the membrane restricts the application of ultrafiltration membranes.^[8] Thus, the requirement of high water flux and anti-protein-fouling membranes led to the necessity of modified CA-based membranes.

Some researchers had blended hydrophilic polymers with ultrafiltration membranes to improve its performance. For instance, Polyethylene glycol (PEG) was selected as a pore-forming additive to prepare modified CA ultrafiltration membrane. During the preparation of membrane, the membrane pore size, porosity, flux and protein rejection could be changed because the membrane-forming system was influenced in phase inversion.^[9] Besides, hydrophilic PEG molecules could create “hydrated layer” around membrane surface, thus modified membrane had beneficial impact in antifouling property.^[10] Some papers also reported that the resistance of protein adsorption of membranes based on the “steric repulsion” effect which was caused by entropic change in free energy.^[11] However, these additives are all miscible in water, which may be leached out in coagulating solution (usually water).^[12] Recently, zwitterions polymers have gradually attracted researchers’ attention in constructing better performance membranes.^[13-15] Membrane modified by zwitterionic polymers displayed non-fouling ability due to the “hydrated layer”, which was fabricated by the charge groups.^[16] Additionally, the “hydrated layer” created by these chains was continuous and close and the result had been revealed by molecular mimicry experiment.^[17] Although antifouling performance of zwitterionic polymers (most of them are long-chains) was improved, the decrease of water flux of membrane which was

attributed to blockage pore of membrane and it had been observed by some researchers.^[18]

Therefore, it needs to find zwitterionic chains with appropriate length to construct good antifouling property of CA membrane without blocking pore of membrane.^[17] Natural amino acids can be applied as grafting modifiers on membrane for its zwitterionic structure and short chains. However, a major bottleneck of CA membrane for modification is the lack of reactive functional groups on the polysaccharides backbones.^[19] Blending CA membrane with polymers containing functional groups can obtain advantageous performance, such as higher flux and better selectivity.^[20, 21] Simultaneously, the functional groups can also be used as reactive site for grafting zwitterionic chains to further improve the antifouling ability of membrane. TEMPO-oxidized cellulose nanofibers (TOCNs), possessing many desirable properties, such as good biocompatibility, reinforcing capability, hydrophilicity, have attracted attention in nanomaterials field.^[22] Significant amounts of carboxylic groups were introduced into native cellulose, maintaining their individual nanofibers morphologies ranged from 3 to 5 nm in width and hundreds μm in length.^[23] A literature has reported that the nano-polysaccharides acids could be further modified through the coupling reaction between the carboxyls and a series of amines.^[24] Therefore, grafting short chain amino acids on TOCNs composite CA membrane can also be achieved in theory.

In this work, lysine could provide amino groups $-\text{NH}_2$ and $-\text{COOH}$ as zwitterionic short-chain and was selected as modifier. TOCNs were blended with CA to fabricate high water flux of composite membranes. Meanwhile, as reinforcing nanofibers, TOCNs also displayed favorable effects for modified membrane in mechanical property due to its nano-structure with higher aspect (length/width) ratios. Then short-chain amino acids were grafted onto TOCNs composite membrane surface to further improve the antifouling capability. From SEM observation, little or even no influence on the morphology and pores structure of membrane was found after grafting short chains. However, the antifouling property of lysine grafted membranes increased without sacrificing water flux and mechanical properties. The lysine modified membranes provided the merits of renewability, biodegradability as well as enhanced properties, behaving great potential for practical application of bio-separation. Considering the current environmental and energy problems, it is a feasible method to decrease the dependency on petroleum based polymers membrane.

2. Experimental

2.1. Materials

Cellulose acetate (CA, Mw 40,000 Da, acetyl content 39.8 %) was purchased from Huibao Chemical Co. (Beijing, China). N, N-Dimethylformamide (DMF) was purchased from Beijing Chemical Works. Lysine and serine were purchased from local chemical reagent companies. Bovine serum albumin (BSA) was obtained from Danielspulber biotechnology Co., Ltd. (Beijing, China). 1-Ethyl-(3-3-dimethylaminopropyl)-carbodiimide hydrochloride (EDAC) and N-hydroxysuccinimide (NHS) were purchased from Sinopharm Chemical Reagent Co., Ltd (Beijing China) and used as received.

2.2. Preparation of TOCNs composite membrane

TOCNs aqueous suspension was prepared using the method reported by others.^[23, 24] Then the TOCNs were dispersed in DMF solvent by vacuum rotary evaporation and solvent exchange. TOCNs composite ultrafiltration membrane was prepared via non-solvent induced phase inversion process. A casting solution containing 15 wt.% CA and 0.75 wt.% (w/w) TOCNs of CA was dissolved in DMF with stirring for 4 h. To obtain homogeneous solution, the casting membrane solution was kept for at least 12 h to get rid of air bubbles. Then, the casting solution was cast on a clean glass plates with a steel knife (250 μm) and the solvent in the cast membrane was subsequently allowed to evaporate for 30 s. After casting, the casting membrane was immersed in a water coagulation bath of deionized water gently. To further reaction and characterization, TOCNs composite membranes were cleaned by deionized water at least 3 times to remove the remaining solvent DMF.

2.3. Reaction of amino acids and blend membrane

TOCNs composite membranes were rinsed in mixed solution (pH 6.0) containing 100 mM EDAC and 50 mM NHS. The pH value of activated solution was adjusted by HCl or NaOH (0.1 M). The carboxyl groups existing in TOCNs were activated at mixing solution for 2 h at room temperature following washed with deionized water to remove unreacted impurities. Then that membranes were immersed in 10mg/ml amino acids (serine and lysine) which had been dissolved in deionized water in advance and, then the pH of solution was adjusted to 8.0 following reacted at room temperature for 12 h. Amino acids functionalized c composite membranes were prepared.

2.4. Membrane structure and properties characterization

2.4.1. Scanning electron microscope (SEM)

The cross-sectional structure of ultrafiltration membranes were frozen in liquid nitrogen, broken, and sputtered with gold before SEM (HITACH S-4800, Japan) analysis.

2.4.2. X-ray photoelectron spectroscopy (XPS)

Membrane surface chemical composition was analyzed by XPS (Thermo Escalab 250XI) using Al K α X-ray source ($h\nu=1486.6$ eV) at a pass energy of 93.9 eV and charge C1s = 284.8 eV for carbon pollution correction. Membrane surface facing the water bath was conducted on the XPS analysis. Survey spectra were run in the binding energy from 0 to 1200 eV, followed by high-resolution scan of the C1s, N1s core-level region XPS spectra of the membranes.

2.4.3. Porosity and mean pore radius of membrane

The porosity (ϵ) was calculated using the following equation:^[25-27]

$$\epsilon = \frac{m_1 - m_2}{A \rho_w} \quad (1)$$

The weights of the wet membranes were first measured and defined as m_1 , then the wet membranes were placed in a vacuum drier at 60 °C for 48 h. The m_2 was the weight of the dry membrane; Where A was the effective area of the membrane (m^2); and l was the membrane thickness (m); ρ_w was the water density ($\text{g}\cdot\text{cm}^{-3}$).

Then the Guerout–Elford–Ferry equation (Eq. (2)) was utilized to calculate membrane mean pore radius (r_m), which was determined by the pure water flux and porosity data: [28, 29]

$$r_m = \sqrt{\frac{(2.7 - 1.75\varepsilon) \times 8\eta l Q_t}{\varepsilon \times A \times \Delta P}} \quad (2)$$

where η was the water viscosity at 25 °C (8.9×10^{-4} Pa s), Q_t was the volume of the permeate pure water per unit time ($\text{m}^3 \text{s}^{-1}$), and ΔP was the operation pressure (0.1 MPa).

2.4.4. Ultrafiltration experiment

Ultrafiltration experiments were conducted under a stirred cell ultrafiltration cup (Amicon 8200, Millipore Co., USA) with volume of 200ml and effective area of 28.7 cm^2 . Membrane was compacted with deionized water for 30min at 0.15 MPa. Then the pressure was adjusted to 0.10 MPa and the water flux (J_{w1}) were calculated by the following equation: [30]

$$J_{w1} = \frac{V}{A \times \Delta t} \quad (3)$$

where V is the volume of permeated solution (L), A is the membrane area (m^2) and Δt is the permeation time (h). Then the 1.0 mg/mL BSA solution was fed into the ultrafiltration cell then maintained at the pressure of 0.1 Mpa for 1 h and the permeation was written as J_p . The rejection (R) of BSA was calculated according to the equation: [31]

$$R_j = \left(1 - \frac{C_p}{C_f}\right) \times 100\% \quad (4)$$

where C_p and C_f (mg/mL^{-1}) refer to the concentration of BSA in permeate and feed solutions, respectively. The concentration of BSA was measured via a UV-vis spectrophotometer at wavelength of 278 nm.

2.4.5. Antifouling experiments of membrane filtration

The membrane fouling behavior was studied and description was presented below. The membrane J_{w1} was measured at 0.1 MPa as formulae 2. Then the membranes were washed with deionized water for 30 min and the pure water flux of the cleaned membranes (J_{w2}) was measured at 0.1 MPa again. Flux recovery ratio (FRR) was introduced for evaluating the antifouling ability of the membranes in brief. The result was calculated using the following expression: [32]

$$FRR = \frac{J_{w2}}{J_{w1}} \times 100\% \quad (5)$$

Further, three ratios were defined to analyse the fouling process of membranes in detail. Here, the degree of total flux loss caused by total fouling is R_t , which defined as the following equation:

$$R_t = 1 - \frac{J_p}{J_{w1}} \quad (6)$$

Specially, R_r and R_{ir} were introduced to distinguish reversible and irreversible fouling, and the R_r and R_{ir} were defined by Eqs. (7) and (8), respectively.

$$R_r = \frac{J_{w2} - J_p}{J_{w1}} \quad (7)$$

$$R_{ir} = 1 - \frac{J_{w2}}{J_{w1}} \quad (8)$$

2.4.6. Contact angle

The contact angle measurement was carried out with a contact angle meter (JC 2000C1, Zhongyi Co., Beijing, China). The frozen dried membrane was first tiled on the platform of contact angle meter, and then 5 μl deionized water was dropped onto the membrane surface. The contact angles were measured from random locations of membrane at least three times and calculated with the software provided by the manufacturer. All the measurements were performed at room temperature.

2.4.7. Zeta electric potential (Zeta)

The membrane surface electro-kinetic characterization was observed via tangential flow streaming potential measurement. Modified membranes were immersed in a 0.001 mol/L KCl solution (in the range of pH 4–9) at room temperature. The zeta potential ζ was calculated by alternative method of determining the zeta potential. [33–35]

2.4.8. Mechanical characterization

After removing water, tensile strength and elongation at break of prepared blend membrane were measured according to CMT4104 electronic universal testing machine with a crosshead speed of 1mm/min. The tested membranes were cut into standard shape with 2 cm effective length and 0.4 cm width stripes. The measurement was performed at 25 °C and 37 \pm 2% relative humidity. Three samples were evaluated and the average values were used.

3. Results and discussion

3.1. TOCNs and TOCNs composite membrane

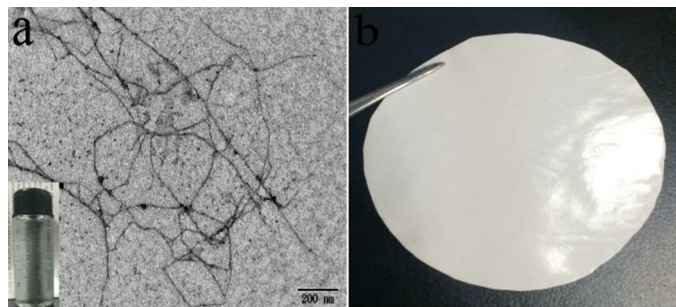


Fig. 1 (a) TEM image of synthesized TOCNs and the inset picture show the dispersion of TOCNs in deionized water; (b) TOCNs composite CA membrane

Fig. 1a presents the TEM of TOCNs dispersing in deionized water. It could be found that mostly individual TOCNs of 3–4 nm in width and a few microns in length, led to nanofibers with high aspect (length/width) ratios of larger than 100. Some papers had reported that the large amounts of selectively formed carboxyl groups present in high densities on the TOCNs surfaces, resulting in the formation of individualized and long nanofibers by electrostatic repulsion.^[23] As shown in the insert picture (Fig. 1a), TOCNs widths were smaller than the wavelength of visible light (780~380nm), thus that nanofibers dispersed in water to be almost transparent. Then TOCNs were blended with CA casting solution to fabricate high water flux membrane. From Fig. 1b, the composite membrane has apparent feature, which are smooth and white surface in morphology, indicating the long filamentous nanofibers could blend into CA film cast solution and prepare membrane successfully.

3.2. SEM characterization Fig. 2 presents the images of the cross-section and the layer of the membranes. It can easily find that all membranes present typical asymmetric structures, consisting of a skin layer and sub-layer with a finger-type structure. A dense spongy structure (Fig. 2a) with a thick skin-layer is formed in CA membrane. The addition of hydrophilic TOCNs apparently promotes the formation of more porous and good interconnection of finger-type structure in the support layer as depicted in Fig. 2e. In addition, a thinner skin-layer (Fig. 2f) can be also observed in the nanofibers composite membrane. The changes in membrane structure could be interpreted by the membrane formation mechanism during phase separation.^[36, 37]

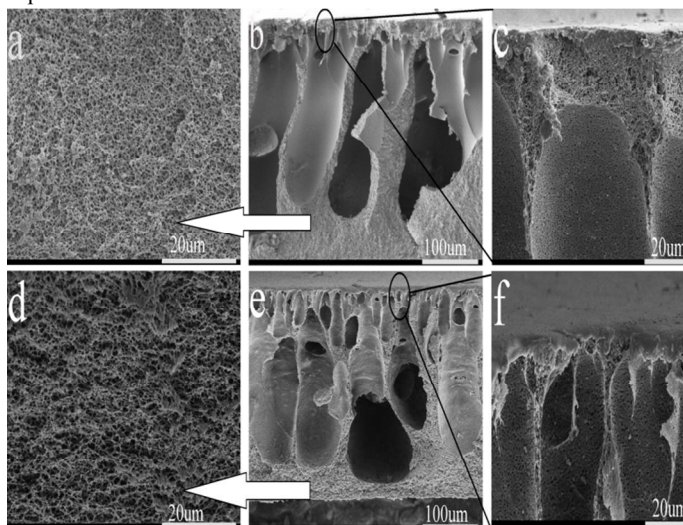


Fig. 2 SEM images of CA membrane (simple named M1) and TOCNs composite membrane (M2). The sub-layer, the cross-sections and the skin layer of M1: (a), (b) and (c); the sub-layer, the cross-sections and skin layer of M2: (d), (e) and (f).

When the cast film solution is immersed into the deionized water, the phase inversion process of preliminary membrane starts because of the low miscibility between the polymer (CA) and the non-solvent (water) in delayed demixing. Meanwhile, the mutual diffusion between water inflow and solvent (DMF) outflow occurs and generates new nucleuses of polymer phase in the casting membrane. Subsequently, the higher concentration of polymer

concentrates on the top layer then the nucleation starts successively in the inferior layer at short time intervals. During the transforming, the free growth of limited nuclei (on the top layer) is prevented, resulting in numbers of small nuclei is developed and then distributes throughout the membrane. Consequently, the formation of big pores is suppressed, and denser membranes (less porous structure) are created.^[38] However, contrary to slow demixing, instantaneous demixing often happens and leads to the acceleration of rate at the thermodynamic unstable system.

As hydrophilic nanofibers, TOCNs accelerate the process of phase separation during membrane formation. Some TOCNs may be leached out of the casting solution with DMF to water and then act as a pore forming agent. Therefore, the membrane-forming system is affected by TOCNs, which increase the thermodynamic instability of the cast film and then result in the formation of big size of pores and more porous structure of M2 (Fig. 2d). Table 1 also presents the porosity and average pore radius (r_m) of the membranes. As shown, the porosity of M2 increases to 84.3%, which is higher than M1 (78.5%) and the average pore radius of nanocomposite membranes is also increased by incorporation of the TOCNs.

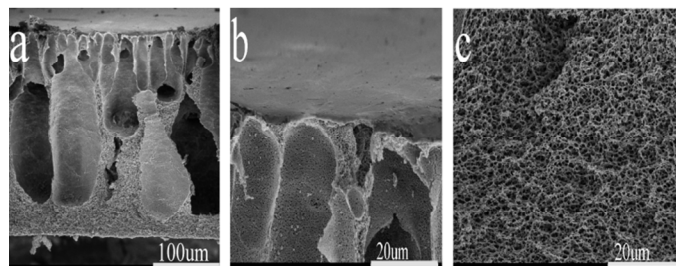


Fig. 3 The cross-sections of lysine modified TOCNs composite membrane (M4): (a); the skin layer: (b) and supporting layer: (c).

F. Nadège et al reported that the functional groups ($-\text{COOH}$) can be further modified by a coupling reaction of the carboxyl with a series of amines,^[25] so it was possible to graft some amines to TOCNs composite membrane. After grafting amino acids on TOCNs composite membrane, as seen in Fig. 3, there were almost no changes in membrane morphology and pores structure compared with M2. Table 1 shows that the porosity and average pores radius of all M2 and M4 are nearly similar. This phenomenon suggests that although some short-chains probably have diffused into membrane cross-section structure, pores inside would not be blocked by grafting short-chains. Similarly, the profiles of porosity and average pore radius for M3 were quite close to that of M2.

Table 1 porosity and average pore radius

Membrane	Porosity (%)	r_m (nm)
M1	78.5	13.8
M2	84.3	41.5
M3	83.7	41.2
M4	84.1	41.5

M1- CA membrane

M2- TOCNs composite membrane

M3- Serine grafted composite membrane

M4- Lysine grafted composite membrane

3.3. XPS characterization

The chemical composition of modified membrane was characterized by XPS analysis. As seen in Fig. 4a, two different characteristic XPS signals for carbon and oxygen were observed at XPS spectra for TOCNs composite membrane. However, after amino acids grafting, one additional emission peak at about 400 eV, which was attributed to N1s, could be observed for M3 and M4. Obviously, amine group was the source of N element for modified membranes. To better observe the surface chemical composition of M4, high-resolution N1s core-level XPS spectrum of M4 analysis was characterized. As shown, two different peaks standing for the NH₂ or NH groups at energy site 399.9 eV and 401.8 eV can be detected in Fig. 4b. Besides, the changes of C1s composition of M2 and M4 were also detected on the high-resolution of C1s in Fig. 4c and Fig. 4d. Three peaks corresponding to binding energies of 284.48, 286.38 and 288.78 eV, which represent the signal of C-C (containing C-H), C-O, and O-C=O species respectively were discovered in Fig. 4c for M2. However, a new signal peak of N-C=O moieties appeared at 287.78 eV when lysine was grafted onto membrane by amide reaction (Fig. 4d).

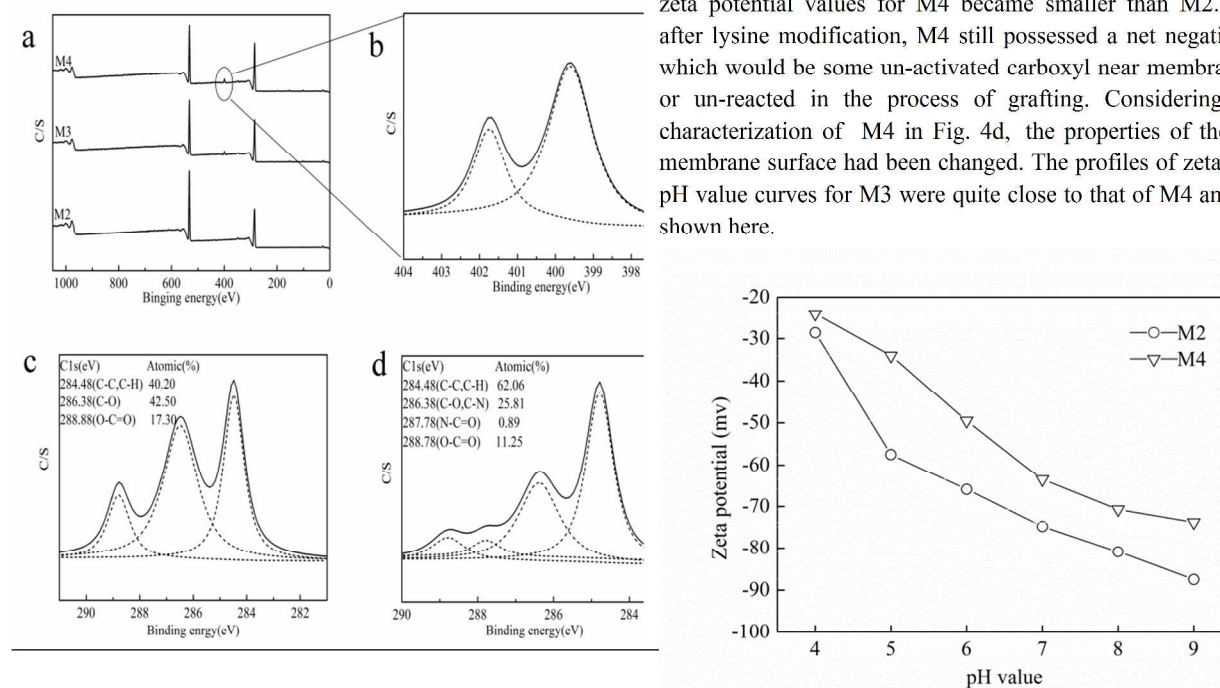


Fig. 4 The XPS analysis of membrane samples: (a) the whole spectra of M2, M3 and M4; (b) the high resolution scans for N1s of M4; the high-resolution C1s of M2: (c) and M4: (d).

In addition, the surface C1s composition was calculated by the quantitative data of XPS analysis. As shown in Fig. 4c, the peak binding energies of 284.48, 286.38 and 288.78 eV had corresponding atomic percentage 40.20%, 42.50% and 17.30%, respectively. However, after lysine grafted on membrane, the percentage of C-C (containing C-H) signal at binding energy of 284.48 eV increased from 40.20% to 62.06%. In contrast, the percentage of C-O signal at 286.38 eV decreased from 42.50% to 25.81%, and the content of O-C=O at 288.78 eV reduced from 17.30% to 11.25%. It may be attributed to the coverage of some amount of lysine on the membrane surface, leading to the change of surface chemical element composition. Although XPS analysis can approximately reach the top 50Å scale of the membrane surface, the obtained data demonstrated that short amino acid chain appeared, at least on the top layer of membrane.

3.4. Zeta-potential measurement

Zeta-potential measurement was introduced to characterize the surface charge properties of membranes. As shown in Fig. 5, the absolute values of zeta-potential increased with increasing pH, and M2 showed higher values than M4 in the whole pH range of 4 to 9. There exist many hydrophilic carboxyl groups in TOCNs composite membrane surface which were facile to be ionized by surrounding water, resulting in negative surface charge under measuring conditions. Clearly, M4 had different absolute zeta-potential value and trends by variation of pH solution, because of Lysine could offer zwitterionic groups containing positive and negative charge after amide reaction with composite membrane. Therefore, the absolute zeta potential values for M4 became smaller than M2. However, after lysine modification, M4 still possessed a net negative charge, which would be some un-activated carboxyl near membrane surface or un-reacted in the process of grafting. Considering the XPS characterization of M4 in Fig. 4d, the properties of the modified membrane surface had been changed. The profiles of zeta potential–pH value curves for M3 were quite close to that of M4 and were not shown here.

Fig. 5 Zeta potential of M2 and M4 measured with varying pH

3.5. Contact angle

Surface hydrophilicity measurement was commonly used to assess the changes in the hydrophilicity and interfacial energy of substrate surfaces.^[39] As one of the most important factors in determining antifouling property, surface hydrophilicity of the membranes was evaluated in this study. Table 2 lists the contact angle of all membranes. It was found that the contact angle decreased significantly after the amino acids modification of membrane compared to M1, which was attributed to the hydrophilic nature of the zwitterionic structure groups. Some papers reported that the decrease of contact angle was corresponded to the elevation of the hydrophilicity, resulting from the enhanced water affinity on the zwitterionic membrane surface. Thus, the close water layer formation will contribute to membrane fouling-resistance.^[16]

3.6. Ultrafiltration characterization

The ultrafiltration experiment of M1 and M2 was conducted to explore water flux and protein flow as the function of time. All of the membranes were compacted with deionized water for 30 min at 0.15 MPa, followed by the measurement of the flux (J_{w1}) at the pressure of 0.10 MPa. As shown in Fig. 6a, M1 had quite low quantitative value whether in aspects of water flux or protein flow. When TOCNs were introduced into membrane, the water flux of M2 increased from 11.8 l/m²h to 123.4 l/m²h, over 10 times increment compared with unmodified CA membrane. The variation of membrane flux should be attributed to the more porous and good interconnection of finger-type structure in the support layer as depicted in Fig. 2e. In addition, a thinner skin-layer, shown in Fig. 2f can also reduce resistance that water flow through the membrane cross-section structure. Although the BSA rejection has slight decrease, the modified membranes have solute rejection of more than 80%, which is effective value for ultrafiltration membrane.

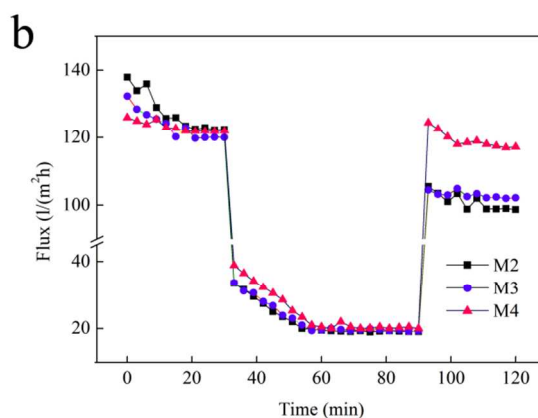
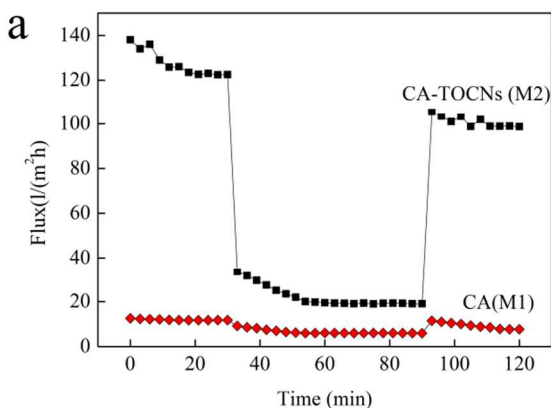


Fig. 6 Ultrafiltration experiments of M1, M2: (a); Ultrafiltration experiments of M2, M3 and M4: (b).

Next, the protein fouling resistance of the prepared membranes was studied. The flux of M2 and amino acids grafted membranes (M3, M4) was plotted against time in Fig. 6b. Because EDAC, NHS and amino acids are small molecular compounds, they could easily diffuse into membrane pore, and the amino acids may graft onto pore surface to some extent. The grafting of amino acids would possibly make the pore size smaller than un-grafted membrane to some extent.^[18] However, the water flux (J_{w1}) of M3 and M4 had little change compared with that of M2 (Fig. 5b), it may be ascribed to the short-chains of serine and lysine. From Fig. 6, it can also be observed that the flux of BSA solution (J_p) was lower than that of pure water flux (J_{w1}) for all the tested membranes. The adsorption and deposition of bio-macromolecules on the membrane surface and/or pore walls result in a distinct decline in water flux with operation time.^[40, 41]

In other words, inevitable pollution by absorption onto surface or blocking pore had occurred at the beginning and would throughout the whole process of experiment. After protein filtration operation, the membranes were rinsed with deionized water for 30min and water flux (J_{w2}) was measured again. During filtration, fouling behavior was simply studied by the water flux recovery rate (FRR) and the results of M1, M2, M3 and M4 were 65.3%, 80%, 85% and 95.9%, respectively, shown in Fig. 7. Clearly, M4 had a better performance in FRR. Further, the considerable membrane fouling could be divided into reversible fouling (R_r) and irreversible fouling (R_{ir}). After lysine modification, as shown in Fig. 5b the flux still maintain a relatively high value and Fig. 7 shows quite higher FRR (95.9%) and lower R_{ir} (4.1%) of M4. Irreversible fouling, which could not be removed by hydraulic cleaning, constituted the primary challenge for membrane modification. As mentioned in Fig. 6b, the results of the R_{ir} value decreased obviously without any influence on pure water flux, which was resulted from the existence of short zwitterionic chains, illustrating the work of antifouling membrane was effective.

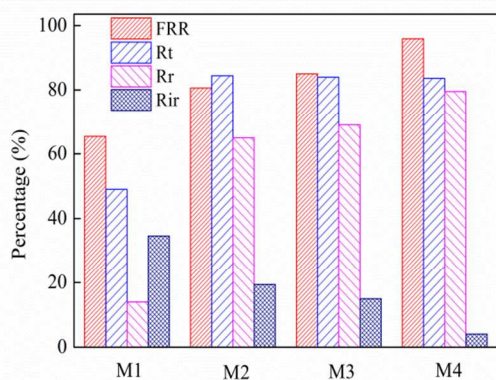


Fig. 7 The evaluation of membranes antifouling of M1, M2, M3 and M4

The suggested anti-fouling mechanism of M4 may be shown in Fig. 8. It is clear that lysine ($\text{NH}_2\text{-(CH}_2\text{)}_4\text{-CH (NH}_2\text{)-COOH}$) is a basic amino acid which contains two amino groups and one carboxylic group. After consuming one amino group in the grafting procedure, lysine grafted on membrane surface could be regarded as zwitterionic groups, which can create “hydrated layer” to resist protein fouling as displayed in Fig. 8. While M3 modified by serine has less ratio of FRR, corresponding lower antifouling performance, because of the membrane modified by serine ($\text{NH}_2\text{-CH-(CH}_2\text{OH)}_4\text{-COOH}$) left single charge -COOH after grafting. Therefore, the FRR of M3 are almost as same as those of M2 which was fabricated by blending TOCNs into CA. Shi et al.^[17] also chemically grafted different kinds of amino acids (lysine, glycine, and serine) onto hydrolysed polyacrylonitrile membrane and found that only lysine modified membrane displayed superior protein anti-fouling ability. Similarly, many researchers had intensively reported the “hydrated layer” created by zwitterionic material and the “zero” fouling or non-fouling mechanism.^[42,43]



Fig. 8 The mechanism of resistance to protein absorption of M4

Table 2 Membrane performance

Membrane	Contact angle (°)	J_{w1}^a	J_{w2}^a	FRR (%)	Rejection (%)
M1	67±2.3	11.8±1.5	7.7±1.2	65.4	93.6
M2	55±1.5	123.4±3.1	98.7±2.6	80.6	85.7
M3	54±2.0	120.2±2.8	102.2±2.7	85.0	86.0
M4	50±2.3	123.0±3.0	118.0±3.1	95.9	86.4

^a The filtration operation was carried out in the pressure of 0.1 MPa and the testing unit all are l/m^2h .

3.7. Mechanical properties

The mechanical properties of the membrane are another consideration for the practical application. From Table 3, it can be found that an overall improvement of both tensile strength and elongation at break due to the introduction of TOCNs. The tensile strength and elongation at break of M2 were increased by 23.9% and 40.4%, respectively. The above impact of TOCNs revealed that the nanofibers have highly reinforcing capabilities, benefiting to the membrane which is under the operation stresses. It is generally accepted that the individual nanofibers have high aspect (length/width) ratios of larger than 100 because of its small width ranged from 3 to 4 nm and long length which is 100–1000 nm.^[23] These excellent characteristics of TOCNs can account for the enhancing mechanical property of composite membrane. After lysine modification, although small amount of decrement was observed in M4, but strengths tensile performance still maintained relatively stable level, indicating that short-chain grafted on membrane had no negative influence on membrane mechanical aspect to some extent. Obviously, the incorporation of TOCNs rendered the modified membranes a promising practical application potential in separation, which is advantage for membrane usually under the operation of stress.

Table 3 Membrane Mechanical properties

Membrane	Tensile strength (MPa)	Elongation at break (%)
M1	3.92	7.06
M2	4.85	9.91
M4	4.78	9.70

4. Conclusion

Herein, a facile way to construct a friendly environment membrane with excellent properties was proposed. Short-chain amino acids, serine and lysine were grafted onto TEMPO-oxidized cellulose nanofiber (TOCNs) composite membrane. The morphologies, chemical compositions, zeta potential, contact angle, ultrafiltration experiment and mechanical properties were characterized. The result shows that physically blended TOCNs with CA could improve flux performance of membranes. And grafting short-chain amino acids onto TOCNs composite membrane chemically could introduce antifouling zwitterionic units on membrane neither changing the cross-section morphologies nor blocking pores structure of membrane. According to the ultrafiltration results, the lysine modified membrane presented good performance both in water flux and anti-fouling. Meanwhile, as reinforce nanofibers, TOCNs also have favorable impact for modified membrane in mechanical property. Thus, we believe this modified membrane, which is biocompatible and beneficial for environmental protection, will have a great potential for practical bioseparation in ultrafiltration membrane field.

^aDepartment of Materials Science and Engineering, Beijing Institute of Technology, Beijing 10008, China.

^bBeijing Engineering Research Center of Cellulose and Its Derivatives, Beijing 10008, China.

*Corresponding author. Tel./fax: +861068940942. E-mail address: dalunbit@163.com (D. Zhang)^cNorth Century

Cellulose Technology Research & Development Co.,Ltd,
Beijing 100081, China.

^dSichuan Nitrocell Co., Ltd, Chendu 610063, China.

References

- [1] Y. Su, C. Mu, C. Li, Z. Jiang, *Ind. Eng. Chem. Res.*, 2009, 48, 3136–3141.
- [2] H.C.S. Chenette, J. R. Robinson, E. Hobley, S.M. Husson, *J. Membr. Sci.*, 2012 423–424, 43–52.
- [3] Y. H. Zhao, K. H. Wee, R. Bai, *ACS Appl. Mater. Interfaces*, 2010, 2, 203–211.
- [4] W.Y Zhou, A. Bahi, Y.J Li, H. Yang and F. Ko, *RSC Advances*, 2013, 3: 11614-11620.
- [5] R. Haddad, E. Ferjani, M.S.Roudeh, A. Deratani, *Desalination*, 2004,167, 403-409.
- [6] R. Ghan, V. Chen, M. P. Bucknall, *Desalination*, 2002, 146, 83-90.
- [7] M. Sivakumar, R.Malaisamy, C.J. Sajitha, D.Mohan b, V.Mohan , R. Rangarajan, *J. Membr. Sci.*, 2000, 169, 215–228.
- [8] R. E. Holmlin, X.Chen, R. G. Chapman, S.Takayama, G. M. Whitesides, *Langmuir*, 2001, 17, 2841-2850.
- [9] M.Sivakumara, D.R. Mohana, R. Rangarajan, *J. Membr. Sci.*, 2006, 268 208-219.
- [10] S. Chen, J. Zheng, L. Li, S.Jiang, *J. Am.Chem. Soc.*, 2005, 127, 14473-14478.
- [11] A. Hucknall, S. Rangarajan, A. Chilkoti, *Adv. Mater.*, 2009, 21, 2441-2446.
- [12] R. Konradi, B.Pidhatika, A. Mühlebach, M. Textor, *Langmuir*, 2008, 24, 613-616.
- [13] S. Chen, F. Yu, Q. Yu, Y. He, S. Jiang, *Langmuir*, 2006, 22, 8186-8191.
- [14] E. Ostuni, R. G. Chapman, R. Erik Holmlin, S. Takayama, G. M. Whitesides, *Langmuir*, 2001, 17, 5605-5620.
- [15] S. Chen, L. Li, C. Zhao, J. Zheng, *Polymer*, 2010, 51, 5283-5293.
- [16] Q. Shi, Y. Su, W. Zhao, C. Li, Y. Hu, Z. Jiang, S. Zhu, *J. Membr. Sci.*, 2008, 319 271-278.
- [17] Q. Shi, Y. Su, W. Chen, J.Peng, L. Nie, L. Zhang, Z. Jiang, *J. Membr. Sci.*, 2011, 366, 398-404.
- [18] L. Ying, P. Wang, E. T. Kang, K. G. Neoh, *Macromolecule*, 2002, 35, 673-679.
- [19] A.G. Boricha, Z.V.P. Murthy, *Chem. Eng. J.*, 2010, 157, 393–400.
- [20] D. Lawrence Arockiasamy, A. Nagendran, K.H. Shobana, D. Mohan, *Sep. Sci. Technol.*, 2009, 44, 398–421.
- [21] C.L. Brousse, R. Chapurlat, J.P. Quentin, *Desalination*, 1976, 18, 137–153.
- [22] T. Saito, Y. Okita, T.T. Nge, J. Sugiyama, A. Isogai, *Carbohydrate Polymers*, 2006, 65, 435-440.
- [23] T. Saito, S. Kimura, Y. Nishiyama, A. Isogai, *Biomacromolecules*, 2007, 8, 2485-2491.
- [24] F.Nadège, M.Suzelei, J. Isabelle, G.Serge, V. Michel R, *Carbohydrate Polymers* 2008, 74, 333-343.
- [25] Y. Chen, Y. Zhang, J. Liu, H. Zhang, K.Wang, *Chem. Eng. J.*, 2012, 210, 298–308.
- [26] V. Vatanpour, S.S. Madaeni, L. Rajabi, S. Zinadini, A.A. Derakhshan, *J. Membr. Sci.*, 2012,401, 132–143.
- [27] J.-F. Li, Z.-L. Xu, H. Yang, L.-Y. Yu, M. Liu, *Appl. Surf. Sci.*, 2009, 255, 4725–4732.
- [28] Y. Chen, Y. Zhang, J. Liu, H. Zhang, K.Wang, *Chem. Eng. J.*, 2012, 210, 298–308
- [29] V. Vatanpour, S.S. Madaeni, L. Rajabi, S. Zinadini, A.A. Derakhshan, *J. Membr. Sci.*, 2012, 401, 132–143.
- [30] T. He, W.Y. Zhou, A. Bahi, H. Yang, F. Ko *Chemical Engineering Journal*, 252, 2014, 327–336.
- [31] H. Ma, B.S. Hsiao, B. Chu, *Polymer*, 2011, 52, 2594–2599.
- [32] Y.Q. Wang, Y.L. Su, X.L. Ma, Q. Sun, Z.Y. Jiang, *J. Membr. Sci.*, 2006, 283, 440–447.
- [33] A. Yaroshchuk, V. Ribitsch, *Langmuir*, 2002a, 18, 2036-2038.
- [34] A. Yaroshchuk, V. Ribitsch, *Langmuir*, 2002b, 18, 2036-2038.
- [35] P. Fievet, M. Sbai, A. Szymczyk, C. Magnenet, C. Labbez, A. Vidonne, *Sep. Sci. Technol.*, 2004, 39, 2931-2949.
- [36] G. R. Guillen, Y.J. Pan, M.H. Li, E. M. V. Hoek, *Ind. Eng. Chem. Res.*, 2011, 50, 3798–3817.
- [37] A. Idris, L. K. Yet, 2006, 280, 920–927.
- [38] R. Abedinia, S. M.Mousavi, R. Aminzadeh, *Desalination*, 2011, 277, 40–45.
- [39] M. Taniguchi, J.P. Pieracci, G. Belfort, *Langmuir*, 2001, 17, 4312–4315.
- [40] A.Nayak, H. Liu, G. Belfort, *Angew. Chem. Int. Ed.*, 2006, 45, 4094–4098.
- [41] J.Y. Park, M.H. Acar, A. Akthakul, W. Kuhlman, A.M. Mayes, *Biomaterials*, 2006, 27, 856–865.
- [42] Y. He, Y. Chang, J. C. Hower, J. Zheng, S. Chen, S. Jiang, *Phys Chem Chem Phys.*, 2008, 10, 5539-5544.
- [43] L. R. Carr, H. Xue, S. Jiang, *Biomaterials*, 2011, 32, 961-968.